24th INTERNATIONAL CONGRESS ON SOUND AND VIBRATION
23–27 July 2017, London

STRUCTURAL DAMAGE DETECTION USING DISTURBED PARTICLE SWARM OPTIMIZATION

Zitian Wei

National Key Laboratory on Ship Vibration and noise, China Ship Scientific Research Centre, Wuxi, China

email: weizitian100@126.com

Jialu Huang and Zhongrong Lu

Department of Applied Mechanics, Sun Yat-sen University, Guangzhou, China.

Wenwei Wu

National Key Laboratory on Ship Vibration and noise, China Ship Scientific Research Centre, Wuxi, China.

An approach based on improved Particle Swarm Optimization (PSO) is proposed to identify structural damages in this study. A disturbance is introduced to avoid premature convergence during evolutionary process. The proposed method pays attention on the mutation of either global or individual best positions in history, aiming to lead the whole swarm to escape from local minima. The feasibility and robustness of the new method are verified by a truss structure. The results show that the proposed method is efficient and effective for structural damage identification and it is not sensitive to measurement noise. A laboratory work is conducted on a beam to verify the effectiveness of the proposed method for damage detection only using the first five natural frequencies.

Keywords: structural damage detection, particle swarm optimization, disturbance, frequency domain, finite element method

1. Introduction

Recently, artificial intelligent algorithms as global optimization methods have been widely used in many research topics including structural damage detection [1-4]. Particle swarm optimization (PSO) as a novel heuristic algorithm has attracted great attentions in the past few years on account of its simplicity, universality and outstanding performances [5-7]. Compared to GA or other optimization algorithms, PSO needs fewer function evaluations. However, similar to some other algorithms, PSO is highly likely to suffer from premature convergence especially in case that problems are complicated and multi-dimensional [8]. Unfortunately, the fitness function for damage detection is complicated and multimodal. Hence, many improvements were proposed to enhance global searching ability of PSO. Kang et al. [9] proposed an immunity enhanced PSO to obtain more accurate identification results in a quicker convergence speed. Sandesh and Shankar [10] utilized a hybrid algorithm combining the advantages of pure PSO and GA for structural damage detection, Jena andf Parhi [11] put forward a modified PSO to identify cracks of cantilever beams. Kaveh and Maniat [12] applied Magnetic Charged System Search and PSO to identify structural damages in frequency domain. Gerist and Maheri [13] investigated a multi-stage approach for damage detection using basis pursuit and PSO.

In this study, a disturbed PSO is proposed for structural damage detection, where a disturbance process is introduced in the original PSO to help the whole swarm enhance the ability to escape from local minima.

2. Methodology for vibration-based damage detection

2.1 Modelling of local damages

Generally, the eigenvalue equation for a finite element model of an intact structure can be expressed as

$$(\mathbf{K} - \omega_j^2 \mathbf{M})\phi_j = 0 \tag{1}$$

where **K** and **M** mean the structural stiffness matrix and mass matrix, respectively. ω_j is the *j*th natural frequency and ϕ_j is the corresponding mode shapes.

When a structure of *nel* elements is damaged locally, the loss in the local stiffness can be evaluated as reduction in local elemental stiffness. The loss in mass can usually be neglected. Therefore, the damaged structural stiffness can be written in the following equation

$$\mathbf{K_d} = \sum_{i=1}^{nel} (1 - d_i)\mathbf{k_i} \tag{2}$$

where $\mathbf{K_d}$ is the damaged stiffness matrix, and $\mathbf{K_i}$ presents the *i*th elemental stiffness matrix. The parameter d_i with value range between 0 and 1 refers to the damage extent of the *i*th element. Therefore, identifying local damages in a structure equals to quantifying the value of the damage parameter vector $\{d\}$.

2.2 Objective function in frequency domain

As to identify the damage index, namely, $\{d\}$, natural frequencies and modal assurance criteria (MAC) are utilized to construct the objective function. The discrepancies of *j*th natural frequencies and MAC can be expressed as

$$\Delta\omega_j = \left| \frac{\omega_j^C - \omega_j^M}{\omega_j^M} \right| \tag{3}$$

$$MAC_j = \frac{(\{\phi_j^C\}^T \{\phi_j^M\})^2}{\left\|\{\phi_j^C\}\right\|^2 \left\|\{\phi_j^M\}\right\|^2} \tag{4}$$

where superscript *C* and *M* mean calculated and measured data, respectively. Thus, the objective function, i.e., fitness value function in PSO, can be assembled by $\Delta\omega$ and MAC as followed.

$$f = \sum_{j=1}^{NF} w_{\omega j} \Delta\omega_j^2 + \sum_{j=1}^{NM} w_{\phi j} (1 - MAC_j) \tag{5}$$

where $w_{\omega j}$ is a weight factor corresponding to *j*th natural frequency, while $w_{\phi j}$ corresponding to *j*th *MAC*. *NF* and *NM* are the numbers of frequencies and mode shapes used in calculation, respectively.

3. Disturbed PSO (DPSO)

3.1 A brief introduction to PSO

PSO is inspired by a model of social interactions in a group of animals seeking for food. An animal which is called a particle in PSO, makes its movement according to the experiences of its own as well as group companions. In the swarm of population of *N*, each particle searches in the D-dimensional space with its location denoted as $\mathbf{x}_i = (x_{i1}, x_{i2}, ..., x_{iD})$. The lower and upper bounds of

*j*th dimension are l_j and u_j. The previous best position of *i*th particle in its own memory is $\mathbf{p}_i = (p_{i1}, p_{i2}, ..., p_{iD})$, while the best position recorded in population movement history, which is shared among the whole swarm is denoted as $\mathbf{p}_g = (p_{g1}, p_{g2}, ..., p_{gD})$. Each particle obtains its new moving velocity by learning $\mathbf{P}_g$ and $\mathbf{P}_i$ at time *t*, which can be formulized below [7]

$$\mathbf{v}_i(t+1) = w\mathbf{v}_i(t) + r_1c_1(\mathbf{p}_i(t) - \mathbf{x}_i(t)) + r_2c_2(\mathbf{p}_g(t) - \mathbf{x}_i(t)) \tag{6}$$

Afterwards, the position of each particle is updated in the following form.

$$\mathbf{x}_i(t+1) = \mathbf{x}_i(t) + \mathbf{v}_i(t+1) \tag{7}$$

where c_1 and c_2 are two positive constants, while r_1 and r_2 are random number between 0 and 1, w is an inertia term, or a weight factor. The most common selection of w is that it decreases from 0.9 to 0.4 with the expression below [7]

$$w = w_{\max} - \frac{w_{\max} - w_{\min}}{T} \times t \tag{8}$$

where $w_{\max}$ and $w_{\min}$ represent initial and final weight, respectively, with T as the maximum number of allowable generations. Meanwhile, a simple treatment is taken to boundary conditions as

$$x_{id} = \begin{cases} l_d & (x_{id} < l_d) \\ u_d & (x_{id} > u_d) \end{cases} \tag{9}$$

In the context of damage detection, l_d=0 means intact status of an element, while u_d=0.99 means the totally destroyed of an element.

3.2 The disturbance process

This study focuses on the crucial factors $\mathbf{P}_g$ and $\mathbf{P}_i$, which determine the movements of each particle. Whether premature convergence happens should be judged at very first. Therefore, a check is necessarily introduced after certain number of iterations.

$$\begin{cases} \left| f^{iter} - f^{iter-M} \right| < \varepsilon \\ f^{iter} > \delta \end{cases} \quad (when\ a \cdot T < iter < b \cdot T) \tag{10}$$

where *iter* stands for the current iteration number. *a* and *b* are the coefficients between 0 and 1 to determine the start and the end of disturbance process. ε and δ are two small tolerances. If Eq. (10) is satisfied, which confirms that premature happens, a disturbance process will be applied on $\mathbf{P}_g$ or $\mathbf{P}_i$, denoted as DG and DI, respectively.

$$DG: p'_{g,d} = p_{g,d} + c_3r_3 \quad (d = 1, 2, ...D) \tag{11}$$

Or

$$DI: p'_{i,j,d} = p_{i,j,d} + c_3r_3 \quad (d = 1, 2, ..., D) \tag{12}$$

where c_3 is the magnitude of disturbance, r_3 is a random number in the range [-1,1]. The subscript ' denotes the disturbed value at current iteration step. Nevertheless, disturbance is not conducted on $\mathbf{P}_g$ and $\mathbf{P}_i$ simultaneously, which will lead to wrong identified results as the disturbance is too strong. It is worthy mentioned that during the disturbance the dimensional value is allowed to exceed the boundary. Simple as the improvement is, it turns out quite effective and efficient, which will be illustrated later in numerical simulation.

The loop of calculation can be concluded in the following steps:

Step 1: Initialize the population (generate a random population of *N* solutions) in the search space.
Step 2: Calculate the fitness values of each particle according to Eq. (5).
Step 3: Update $\mathbf{P}_g$ and $\mathbf{P}_i$.
Step 4: If Eq.(10) is satisfied, conduct disturbance according to Eqs.(11) or (12).
Step 5: Evolve each particle's position according to Eqs. (6) and Eq. (7).
Step 6: Treat the boundary using Eq. (9).
Step 7: Repeat Step 2 to 6 until the maximum number of iterations is reached.

4. Numerical simulation

4.1 Parameters setting

The parameter *w* in Eq. (8) decreases from 0.9 to 0.4 linearly. c_1 and c_2 are both set to be 2.0 in Eq. (6). Population *N* is 100. $w_{\omega j}$ and $w_{\phi j}$ in Eq. (5) are both set to be 1. Parameters in Eq. (10) are *M*=15, *a*=1/3, *b*=2/3, $\varepsilon = 10^{-4}$ and $\delta = 10^{-6}$. Disturbance amplitude c_3 equals to 0.1.

Original PSO and GA (GA function in MATLAB®) are introduced as comparison. 10 runs are performed for each algorithm in the damage case. To simulate measurement noise, the natural frequencies and mode shapes are contaminated with 1% and 10% noise, respectively.

4.2 A truss structure

A 26-bar truss in Fig. 1 is studied. The length of each exterior bar is 1m. each bar shares the same section area, 0.004m^2. Young's modulus *E* is 200GPa, while mass density $\rho = 7800\,\mathrm{kg/m^3}$. The total number of elements and nodes are 26 and 12, respectively. Assumed damages are located at 1st, 6th, 12th, 13th and 23rd elements with reduction in stiffness of 10%, 30%, 23%, 40% and 35%, respectively. These 4 algorithms share the same iteration number, 300, in each run.

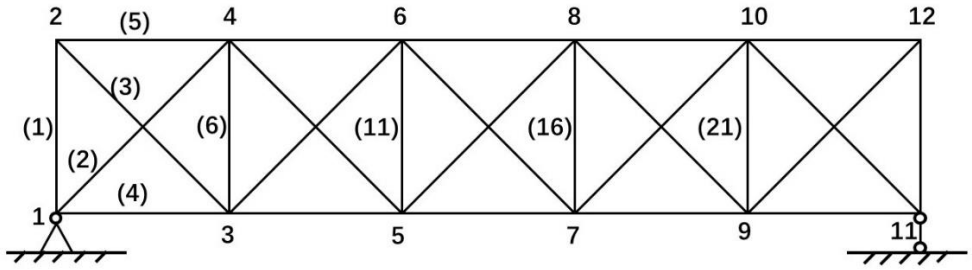

Figure 1 a 26-bar truss

4.2.1 Comparisons with GA and original PSO

Comparisons with GA and original PSO are performed to illustrate the effectiveness, robustness and superiority of proposed methods. First 3 frequencies and mode shapes are utilized. Figure 2 shows the damage detection results in noise-free condition. Black asterisks represent true values. The lines with small rings are the averaged detection results of 10 runs, while the vertical segment line at each ring denotes the maximum and minimum of each element in 10 runs, respectively. It can be observed that GA locates damages with several misidentifications. Original PSO fails to locate the damages correctly due to premature convergence in some runs, which can be judged by the lengths of segments. Fortunately, DG and DI-PSO succeed in identifying damages without any error. The two improved methods are more accurate and less time-consuming than GA.

Figure 3 shows when frequencies and mode shapes are polluted by noise, DG-PSO and DI-PSO are still able to obtain quite desirable identification results in each run, which are superior to GA in identifying damage extents. Failures in identification of damage index by original PSO in some runs directly lead to unsatisfactory results with several large misidentifications. It can be found that in this case, GA, DG-PSO and DI-PSO perform more steadily than original PSO, while DG-PSO and DI-PSO show better performance and less false alarms than GA and original PSO.

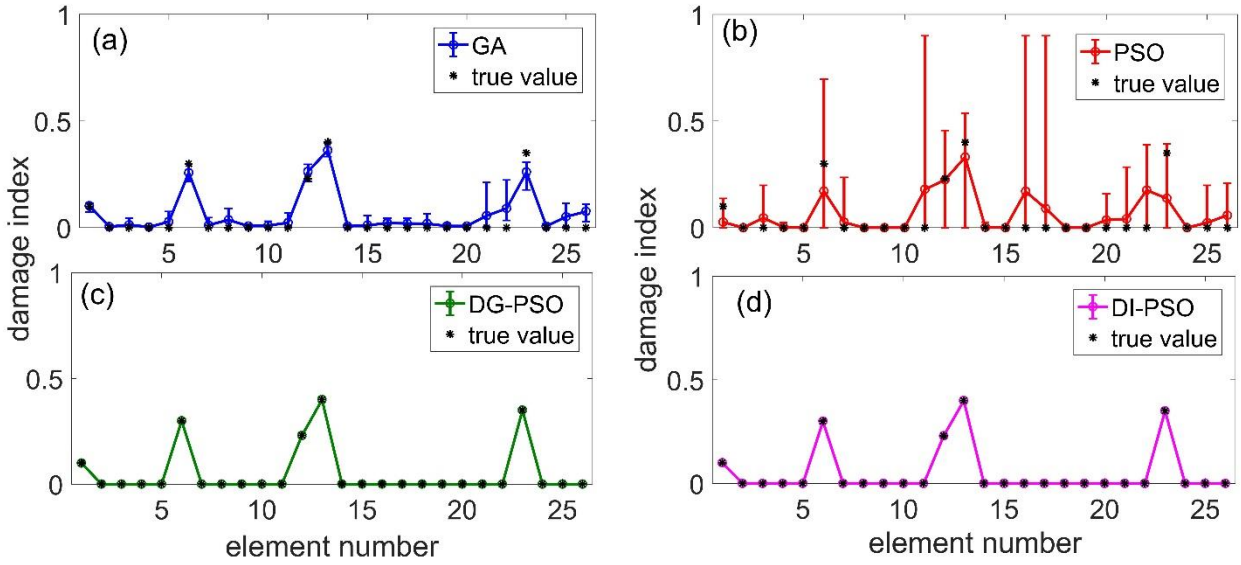

Figure 2 damage detection results of the truss without noise

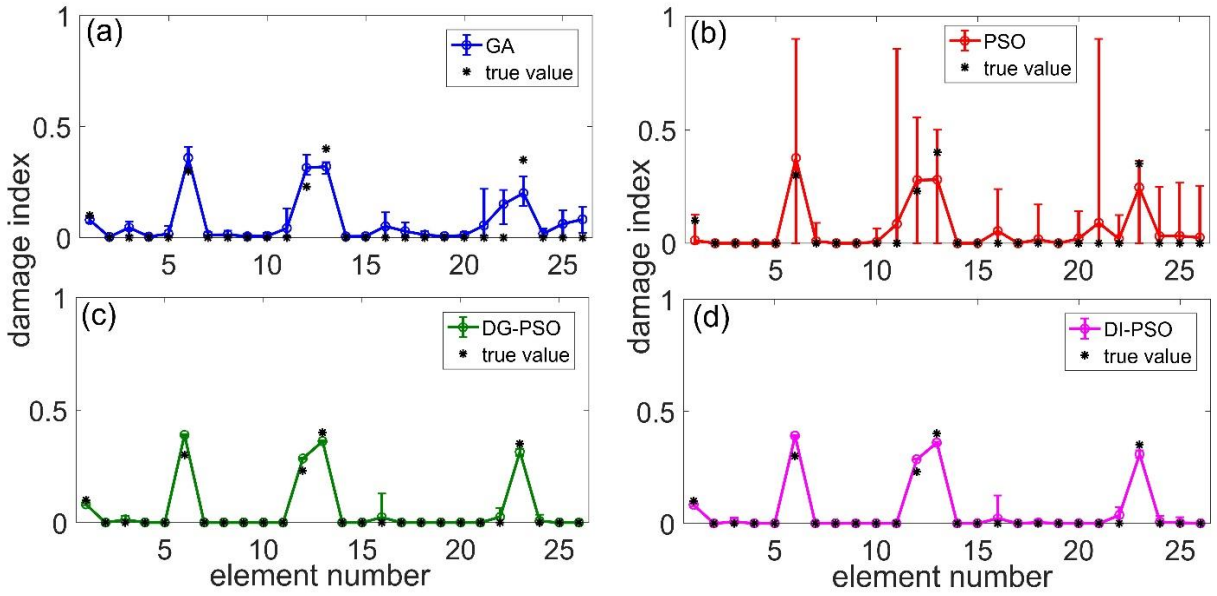

Figure 3 damage detection results of the truss with noise

4.2.2 Analysis of DG-PSO and DI-PSO

The characteristics of DG- and DI-PSO are going to be analysed in noise-free condition. One run is selected as representative to show the evolutionary processes of fitness values and damaged elements. It can be viewed from Fig. 4 that on one hand, disturbance help elements, like element 1, 6, 12 in DG and element 6 in DI, to escape from local minima and re-find the right values. One the other hand, some elements like element 23 in DG and element 23 in DI, which has already found the right values before disturbance, are not affected by subsequent disturbance processes.

The evolutionary processes of fitness values calculated by GA, DI-PSO and DG-PSO are illustrated in logarithmic form in Fig. 5. The final converged best fitness values from both DG and DI are both smaller than 10^{-15}, which indicates the robustness of proposed methods. It can be discovered that in absence of premature convergence, PSO-based methods are prior to GA in convergence precision. It can also be observed that from Fig. 2 to Fig. 5 that DG-PSO and DI-PSO have the equivalent ability of leading whole population to escape from local minima and seek out the global optimization in case of premature convergence.

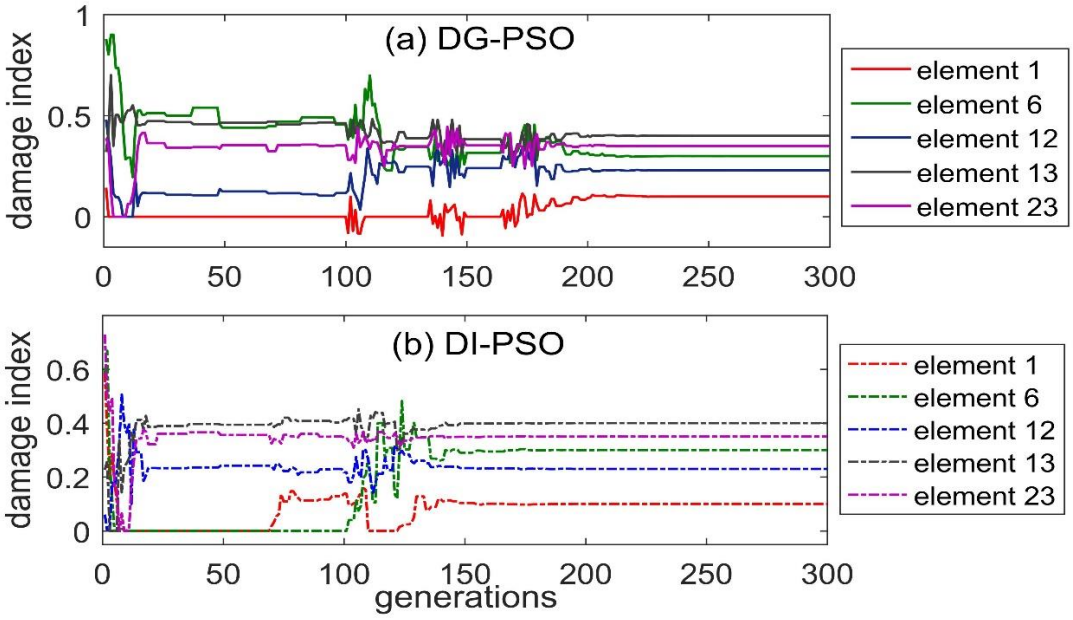

Figure 4 evolutionary processes of damaged elements by DG-PSO and DI-PSO without noise

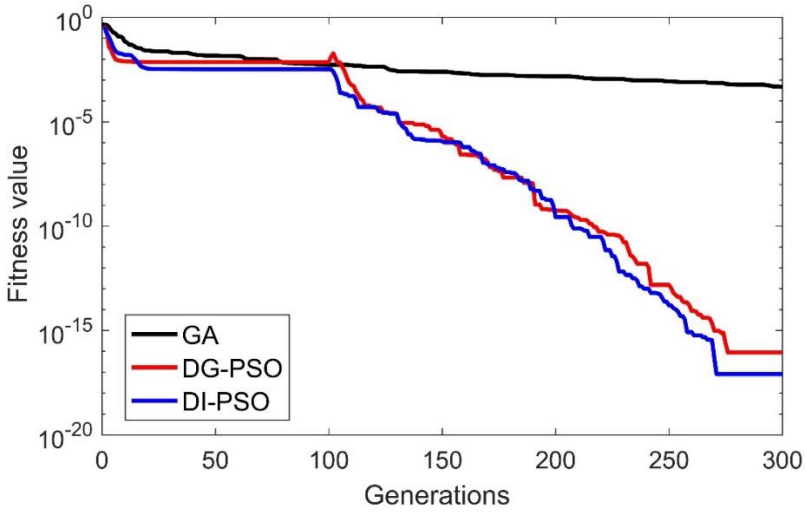

Figure 5 evolutionary processes of fitness values without noise

5. Laboratory work

The proposed method is further demonstrated with laboratory work of a free-free steel beam shown in Fig. 6. The beam is hung by two nylon ropes at two ends. The parameters of the beam are: length 2.1m, width b=0.025mm and height $h_0 = 0.019\text{m}$, the elastic modulus and mass density of the material are 207GPa and 7832kg/m^3, respectively. The damage is simulated by a crack located at 1.72m from the left free end, created by a machine saw with 1.3mm thick cutting blade. The crack depth d_c is 3mm. An impulsive force was applied with an impact hammer model B&K 8202 at 1.2 m from the left end. The sampling frequency is 2000Hz. Four-second acceleration response data are collected. An accelerometer model B&K 4370 at the mid-span of the beam are used to extract the first five natural frequencies of the intact and damaged beam for damage identification. The first 5 natural frequencies of the intact and the damaged beam with crack are shown in Table 1.

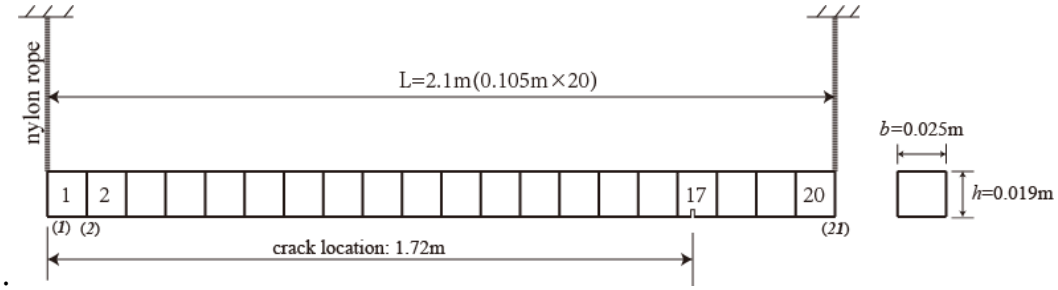

Figure 6 Sketch of the experimental beam (dimensions are not scaled)

The beam is discretized into 20 Euler beam elements. The crack locates at the 17th element in the finite element model. The natural frequencies calculated from the finite element model are quite close to the measured values, which indicates that the initial finite element model is accurate enough for the subsequent damage identification.

Table 1 Modal frequencies of beam from test and analytical results and relative error(%)

Modal frequency		1st	2nd	3rd	4th	5th
Intact	Measured	22.868	62.763	123.049	203.236	303.452
	FEM	22.771(*-0.4*)	62.763(0.0)	123.044(*0.004*)	203.419(*0.09*)	303.934(*0.16*)
Dam-aged	Measured	22.797	62.622	122.559	202.271	302.490
	DG-PSO	22.758(*-0.17*)	62.623(*0.002*)	122.501(*0.05*)	202.304(*0.016*)	302.508(*0.006*)

As only the measured natural frequency data are used in the damage identification, only the first term in the objective function i.e., Eq.(5), is used. DG-PSO is utilized here with iterations of 500 in each of 10 runs. Figure 7 shows the identified result. One can find that the location of the damage has been identified successfully, and the identified extent of damaged element 17 is 5.66%. The true damage value is obtained by a direct identification with the assumption that location of damaged element is known and other elements are intact. It is found to be 9.5%.

Figure 7 shows that there are 2 large false identifications in element 3 and 18. The false alarm in element 3 may be due to the reason that it is the symmetric one of element 17. The false alarm in element 18 can be explained since element 18 is in immediate adjacent to the damage and the vibration energy in the element would be much more disturbed than those in other elements as discussed by Shi and Law [14]. The natural frequencies of the beam calculated with the identified parameters are shown in Table 1 and they are found matching the experimental values very well indicating the success of the identification.

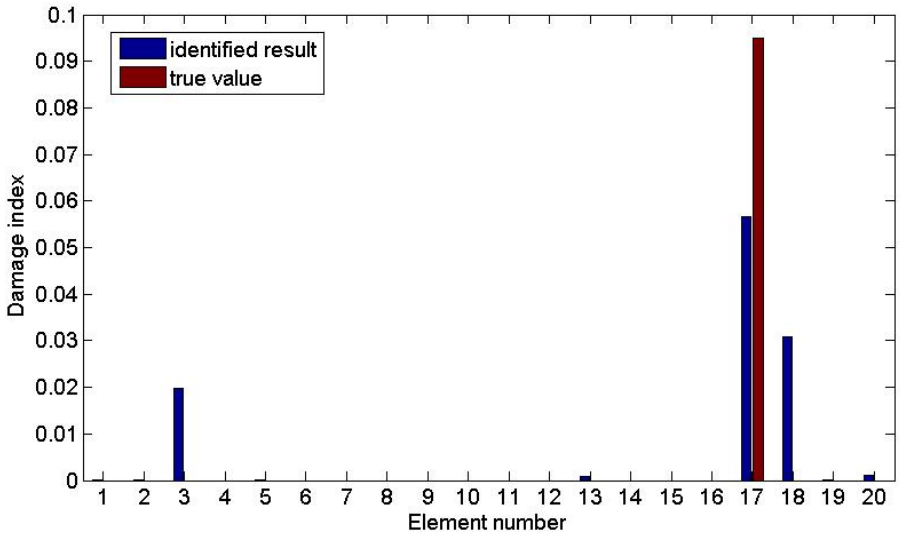

Figure 7 damage identification result of the experimental beam

6. Conclusion

Damage detection approach based on disturbed PSO using vibration data is proposed. A disturbance process is introduced to avoid premature convergence by helping particles to escape from local minima. A truss structure in numerical simulation and a laboratory work are utilized to illustrate the robustness, effectiveness and efficiency of the proposed methods. Only first few natural frequencies and mode shapes are needed in structural damage identification even in noise-polluted condition. It indicates the proposed method has potential for real applications.

REFERENCES

1 Xu, H. J., Ding, Z. H., Lu, Z. R., and Liu, J. K., Structural damage detection based on Chaotic Artificial Bee Colony Algorithm. *Structural Engineering and Mechanics*, **55**(6), 1223-1235, (2015).

2 Vakil-Baghmisheh, M.T., Peimani, M., Sadeghi, M.H., Ettefagh, M. M., Crack detection in beam-like structures using genetic algorithms. *Applied Soft Computing.* **8**(2), 1150-1560, (2008)..

3 Chou, J. H., Ghaboussi, J. Genetic algorithm in structural damage detection. *Computers & Structures*. **79**(14), 1335-53, (2011).

4 Xu, H. J., Liu, J. K., and Lu, Z. R., Structural damage identification based on Cuckoo Search Algorithm. *Advances in Structural Engineering*. **19**(5), 849-859, (2016).

5 Kennedy, J, Eberhart, R., Particle swarm optimization. *Proceedings of Proceedings of IEEE international conference on neural networks*. Perth, Australia, 27 Nov.-1 Dec. (1995).

6 Eberhart, R. C., Kennedy, J. A new optimizer using particle swarm theory. *Proceedings of Proceedings of the sixth international symposium on micro machine and human science*. New York, USA, (1995).

7 Shi, Y. H., Eberhart, R. A., modified particle swarm optimizer. *Proceedings of Evolutionary Computation Proceedings, IEEE World Congress on Computational Intelligence*: *IEEE*, (1998).

8 Seo, J-H, Im, C-H, Heo, C-G, Kim J-K, Jung H-K and Lee C-G. Multimodal function optimization based on particle swarm optimization. *IEEE Transactions on Magnetics*. **42**(4), 1095-98, (2006)

9 Kang, F, Li, J. J., Xu, Q. Damage detection based on improved particle swarm optimization using vibration data. *Applied Soft Computing*. **12**(8), 2329-35, (2012).

10 Sandesh, S. and Shankar, K., Application of a hybrid of particle swarm and genetic algorithm for structural damage detection, *Inverse Problems of Science and Engineering*. **18**(7), 997-1021, (2010).

11 Jena, P. K. and Parhi, D. R., A modified particle swarm optimization technique for crack detection in cantilever beams. *Arabian Journal for Science and Engineering*. **11**, 1-10, (2015).

12 Kaveh, A. and Maniat, M., Damage detection based on MCSS and PSO using modal data, *Smart Structures & Systems*. **15**(5), 1253-1270, (2015).

13 Gerist, S, and Maheri, M. R., Multi-stage approach for structural damage detection problem using basis pursuit and particle swarm optimization. *Journal of Sound and Vibration*. **384**, 210-226, (2016).

14 .Shi, Z. Y. Law, S. S, Zhang, L. M., Structural damage detection from modal strain energy change, *Journal of Engineering Mechanics* **126**(12), 1216-1223, (2000).